HETEROCYCLES, Vol. 65, No. 10, 2005, pp. 2395 - 2409
Received, 23rd June, 2005, Accepted, 15th August, 2005, Published online, 23rd August, 2005

1,3-BENZODIOXOLE-BASED β- AND γ-PEPTIDE LINKAGES EXHIBITING UNIQUE FLUORESCENCE, CONFORMATION, AND SELF-ASSOCIATION PROPERTIES

Masaya Suzuki,[a,b] Yuya Ohguro,[a] Kazukiyo Kobayashi,[a] and Yoshihiro Nishida[a]*

[a]Department of Molecular Design and Engineering, Graduate School of Engineering, Nagoya University, Chikusa-ku, Nagoya 464-8603, Japan, E-mail: nishida@mol.nagoya-u.ac.jp
[b]Research and development, Tokai Optical Co., Ltd., 5-26 Shimoda, Eta-cho, Okazaki 444-2192, Japan.

Abstract – Four types of β- and γ-peptide models were prepared from our previous asymmetric 1,3-benzodioxole and characterized by means of fluorescence and ^{1}H NMR spectroscopy. A β-peptide model carrying secondary amide linkages at both of the *C*- and *N*-termini took a rigid coplanar conformation, emitting the strongest fluorescence [Ex.(max) 340 nm and Em.(max) 424 nm] among the four models. Dual intra-molecular hydrogen bonds were associated with the stable coplanar conformation. A tertiary β-peptide model carrying a tertiary amide linkage at the *C*-terminus took a twisted conformation around the *C*-terminal to afford a pair of rotational isomers (atropisomers) detectable with ^{1}H NMR spectroscopy. Both secondary and tertiary γ-peptide models showed a notable self-association property to afford dimers made of complementary intra- and intermolecular hydrogen bonds.

INTRODUCTION

1,3-Benzodixoles constitute a backbone of many plant products showing remarkable antioxidant and antibacterial activities.[1] The rigid bi-cyclic structure as well as the notable biological potential have provided major bases to the molecular design of 1,3-benzodioxole-based bio- and chemo-functional compounds.[2] Also in our preceding studies,[3] we designed asymmetric 1,3-benzodioxole-4-carboxylates

having a stereogenic center at the C-2 position. More recently,[4] the asymmetric skeleton of compound (**1**) was extended to bi-functional 1,3-benzodioxoles [(**2a**) and (**2b**)] which carry also a nitro group (Scheme 1). Since the nitro group is a convenient amino group precursor, a series of artificial peptide linkages can be assembled from the bi-functional 1,3-benzodioxoles. We have already seen that some of 5-acylamide derivatives such as **3a** emit visible fluorescence (Ex. 340 nm, Em. 400~550 nm) under UV light though the 5-nitro derivatives are non-fluorescent. The X-Ray diffraction studies have shown that the fluorescent amide derivatives take a rigid coplanar conformation due to intramolecular hydrogen (H) bonds.[5,6] These results have supported that the bi-functional 1,3-benzodioxoles are useful for assembly of bio- and chemo-functional conjugates, and the utility is being evaluated in application studies.[7,8]

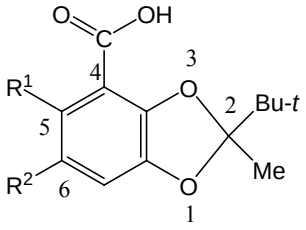

1: $R^1 = R^2 = H$

2a: $R^1 = NO_2$, $R^2 = H$

2b: $R^1 = H$, $R^2 = NO_2$

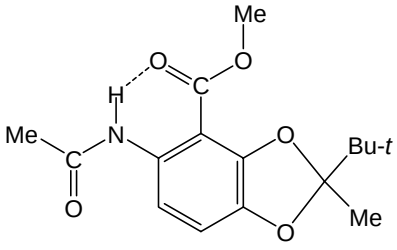

3a

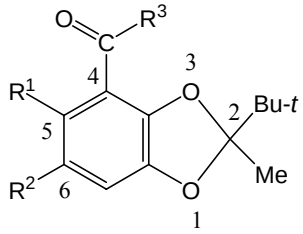

4a: R^1 = NHAc, $R^2 = H$, R^3 = NHPr
5a: R^1 = NHAc, $R^2 = H$, $R^3 = NEt_2$
4b: $R^1 = H$, R^2 = NHAc, R^3 = NHPr
5b: $R^1 = H$, R^2 = NHAc, $R^3 = NEt_2$

Scheme 1 Bi-functional 1,3-benzodioxoles [(**2a**) and (**2b**)] and the four types of peptide models [(**4a)**, **(4b**), (**5a**)**,** and (**5b**)] examined in this study.

In the present study, we examined the fluorescence and conformation properties of four types of peptide models [(**4a**), (**4b**), (**5a**), and (**5b**)]. The peptide models examined here carry an acetamide (NHAc) group at the *N*-terminal and either *n*-propylamide or diethylamide group at the *C*-terminal. Although they are made of such small amide linkages, they each show a highly unique fluorescence, conformation, and self-association property, which will key bases to the design of higher bio- and chemo-functional conjugates.

RESULTS AND DISCUSSION

*1. Syntheses of the four β- and γ-peptide models from **1***

The four peptide models were prepared starting from **1**[9] (Scheme 2). The 4-carboxyl group was condensed with *n*-propylamine or diethylamine to give the corresponding secondary and tertiary amide

compounds [(**6**) and (**8**)]. Each of the amide compounds was treated with nitronium tetrafluoroborate[10] to introduce a nitro group. We found here that site-selectivity in the nitration reaction was different from the case of **1** which gave **2a** and **2b** in 7: 3.[4] From **6**, 5-nitro compound (**7a**) was derived in a site selective way (**7a**: **7b** = 95: 5), while a mixture of **9a** and **9b** was derived from **8** in a non-selective manner (55:45). These results have shown that the site selectivity changes depending on the types of 4-carbonyl group. The conformations and π-electron conjugated structures which are different among these substrates may have certain influences. These reactions gave no 7-nitro compound in any cases. Each of the products was purified with silica gel column chromatography, and the nitro group was reduced by catalytic hydrogenation. The derived amino group was *N*-acetylated with acetic anhydride to afford the four models [(**4a**), (**4b**), (**5a**), and (**5b**)]. These models were used without optical resolution.

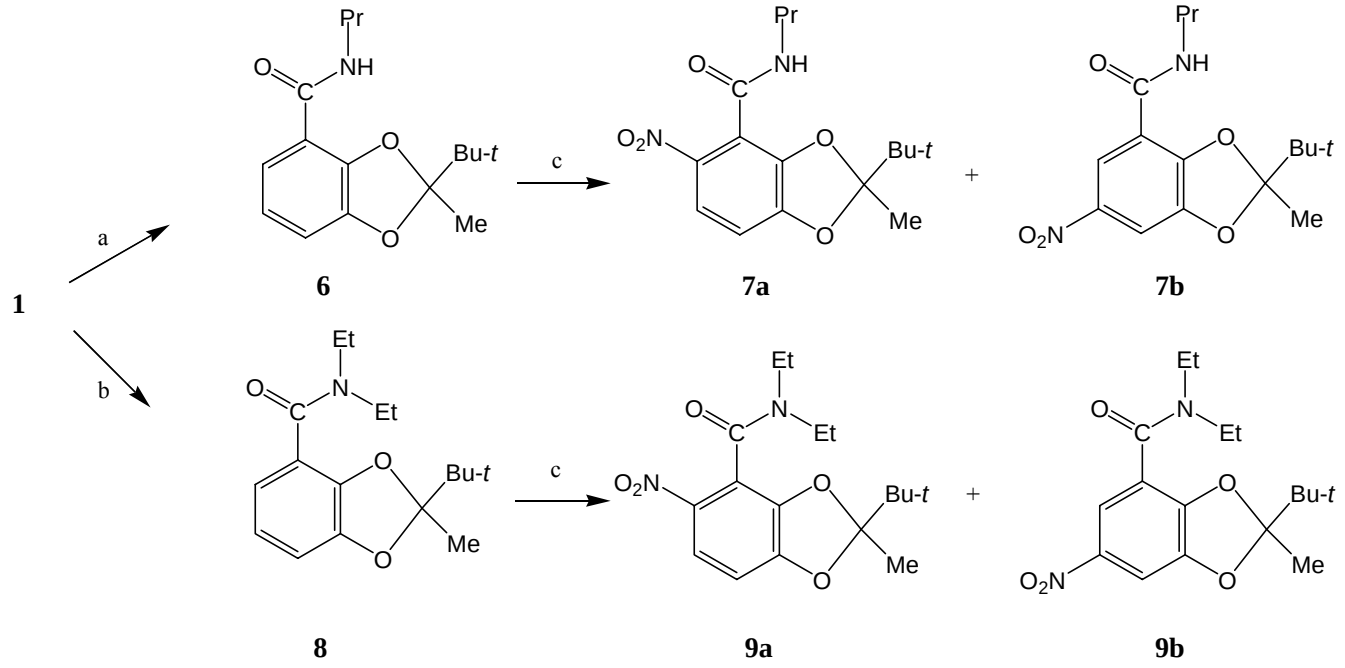

Scheme 2 Synthesis of peptide precursors. Reagents: a) HFPDA in toluene, *n*-propylamine/ DMAP/ Et_3N in CH_2Cl_2, b) HFPDA in toluene, diethylamine/ DMAP/ Et_3N in CH_2Cl_2, c) NO_2BF_4 in MeCN.

*2. Strong fluorescence and rigid coplanar conformation of β-peptide model (**4a**)*

As shown in Figure 1, every peptide model is fluorescent though the intensity and wavelength are different among the four types. The β-peptide model (**4a**) gave the strongest fluorescence which allowed highly sensitive detection (< 10^{-12} M) by fluorescence spectroscopy (*ca*. 90 % quantum yield of quinine sulfate). The UV spectroscopy has shown that this model possesses a longer π-electron conjugation

structure than the other ones. Similarly to **3a**, **4a** may take such a rigid coplanar conformation allowing the 4-carbonyl group to conjugate with an aromatic π-electron system and form an intramolecular H-bond. The strong fluorescence of **4a** seems to arise from the rigid coplanar conformation.

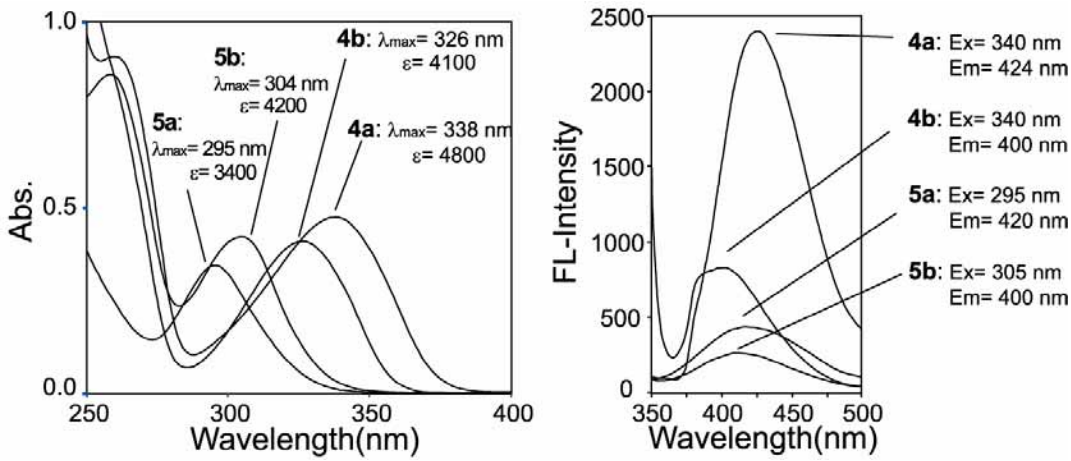

Figure 1. UV and fluorescence (FL) spectra of the four peptide models in MeOH solutions [Concentrations: 1.0 x 10^{-4} M (UV) and 1.0 x 10^{-7} M (FL) (**4a** and **4b**). For **5a** and **5b** having weak fluorescence, the fluorescence spectra measured at 1.0 x 10^{-6} M are given].

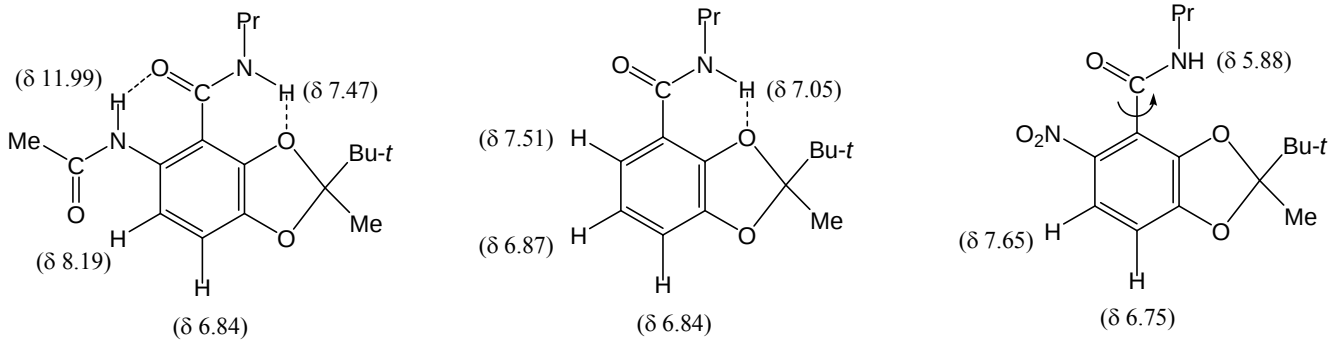

4a **6** **7a**

Figure 2. Selected ^{1}H NMR chemical shifts of secondary β-peptide models (500 MHz, $CDCl_3$, 25 °C)

In ^{1}H-NMR spectroscopic analysis ($CDCl_3$), the two amide protons (–CO-N<u>H</u>-) in **4a** gave broad singlet signals. As summarized in Figure 2, the 4-CO-N<u>H</u>- signal (7.47 ppm) of **4a** shifted to a closer region to the same proton signal of **6** (7.05 ppm) rather than to that of **7a** (5.88 ppm). The observed down-field shift indicates that the 4-CO-NH- proton is associated with an intra-molecular H-bond with *O*-3 atom. The

coplanar amide conformation involving the intra-molecular H-bond is characteristic of 1,3-benzodioxole-4-carbamides like compound (**6**).[3] In the case of **4a**, the 5-NHAc group was found to stabilize the coplanar conformation: the 4-CO-NH- signal shifted to a more down field region than **6**. In the case of **7a**, however, the 5-nitro group has an electron static repulsion with the 4-carbonyl group, and the coplanar geometry is distorted.

These ^{1}H NMR spectral data allowed us to assume that **4a** has another intramolecular H-bond around the *N*-terminal linkage. As shown previously with **3a** (Scheme 1), 5-acylamide derivatives form an intra-molecular H-bond between 5-NH- and 4-C=O atoms.[4,5] The 5-NH-CO signal of **3a** shifted to a highly down-field (10.62 ppm), indicating that the amide proton is associated with the intra-molecular H-bond. The 5-NH-CO signal of **4a** was further de-shielded (11.99 ppm), showing the presence of a more stable H-bond in the coplanar conformation. In the case of the other peptide models [(**5a**), (**4b**) and (**5b**)], the 5-NH-CO signals shifted to a region between 8.2 and 8.6 ppm, showing that they have no intra-molecular H-bond (Figures 3 and 5).

It is evident that the resultant dual intramolecular H-bonds in **4a** work in a complimentary way for stabilizing the coplanar conformation around the amide linkages. The rigid coplanar structure should be related with the strong fluorescence as observed in Figure 1. We have seen also that the fluorescence of the related water-soluble amide compounds holds the strong intensity in a wide range of pH, in interactions with receptor proteins, and also after photo-irradiation.[7,8] We will show in this paper that the secondary β-peptide (**4a**) possesses no self-association property in $CDCl_3$, while the other models have a notable property. This means that the two amide groups used in the dual intra-molecular H-bonds can participate in neither homo- nor heterogeneous inter-molecular H-bonding associations in solutions.

*3. Atropisomers from tertiary β-peptide models [(**5a**) and (**9a**)]*

As shown in Figure 1, the UV absorption band (π -π^*) of **5a** is blue-shifted in comparison with the band of **4a**. Obviously, the π-electron conjugation is different between **4a** and **5a**. Probably, the 4-carbonyl group in **5a** can not take the coplanar conformation due to the bulky tertiary amide group. The ^{1}H NMR spectral data supported this assumption. The 5-NH-CO signal shifted to an upper-field (8.12 and 8.36 ppm) in comparison with **4a** (11.99 ppm). The chemical shift means that **5a** has no intramolecular hydrogen bond between 4-C=O and 5-NH groups. Also the H-6 signals (7.28 and 7.30 ppm) shifted to an upper-field, indicating that the conformation at the 5-NHAc moiety is also deviated from the rigid coplanar one taken **4a**. Of more significance was the result that the ^{1}H NMR signals of **5a** were highly broadened and split into two peaks (Figure 4). The result suggested the presence of isomers in **5a**.

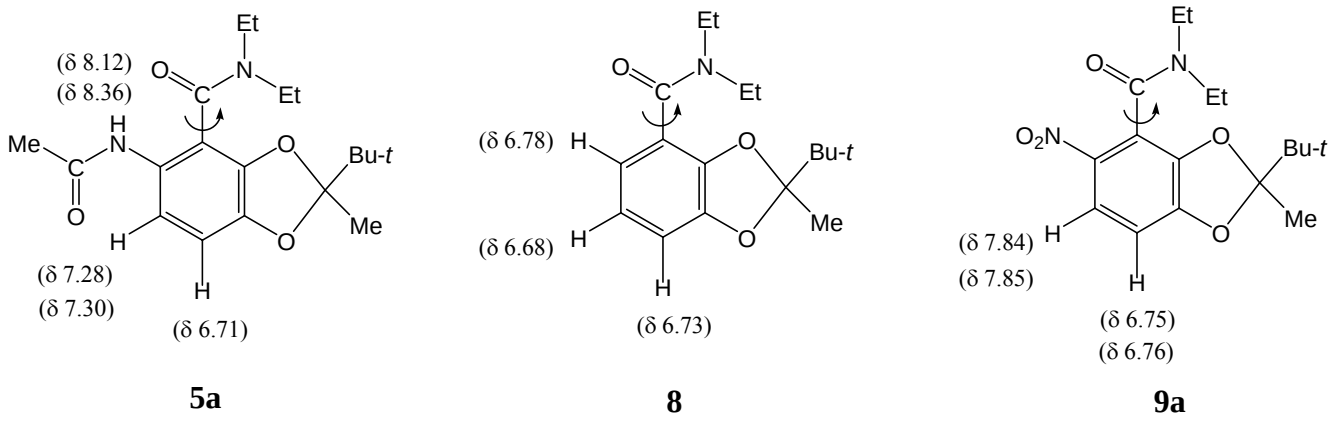

5a **8** **9a**

Figure 3. Selected ^{1}H NMR spectral data of **5a** and the related tertiary β-peptide models [(**8**) and (**9a**)] (500 MHz, $CDCl_3$, 25 °C)

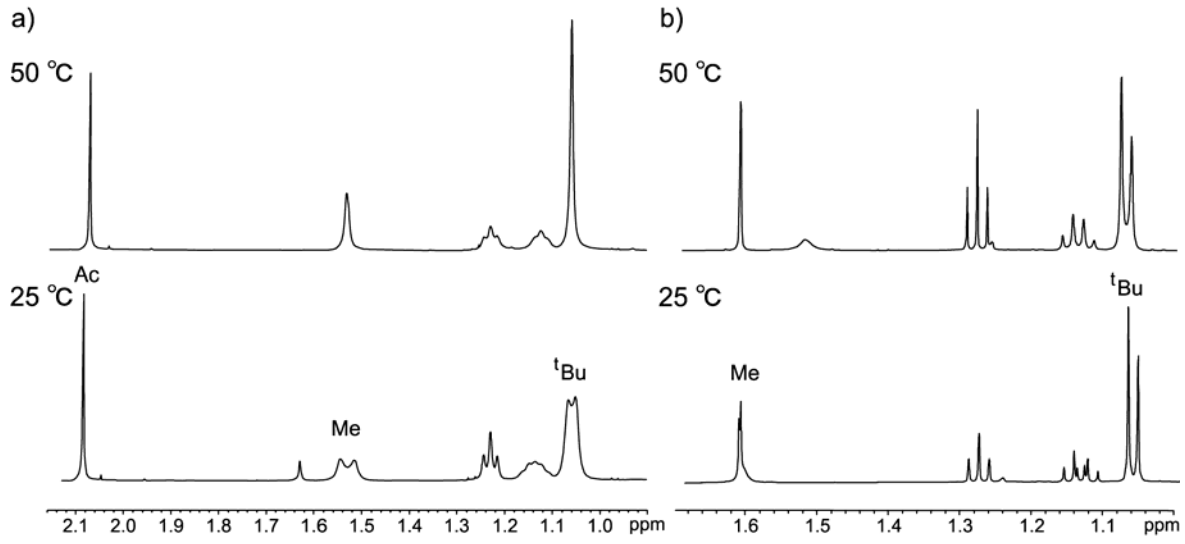

Figure 4. ^{1}H NMR spectra of **5a** (left) and **9a** (right) measured at 25 and 50 °C (500 MHz, $CDCl_3$)

At elevated temperatures, the split signals were unified. This observation means that **5a** gives a pair of inter-convertible isomers. 5-Nitro compound (**9a**) also gave two isomers in the ratio of *ca*. 3:2 (Figure 4b), and every signal was sharper than those of **5a**. On the other hand, compound (**8**) having no C-5 substituting group did not give such isomers. These results indicate that the two isomers arising from **5a** and **9a** are rotational isomers which are called atropisomers.[11] It is highly probable that the free rotation around a Ph-C=O single bond is restricted by the neighbouring groups (*O*-3 and 5-NHAc or 5-NO_2). This is because bulky tertiary benzamides[12] and benzanilides[13] are reported give similar isomers.

Though the atropisomerism can not be evidenced easily with ^{1}H NMR spectroscopy, the asymmetric 1,3-benzodioxole skeleton enables us to detect the isomers as a pair of diastereomers. For the peptide model (**5a**) which gave unified ^{1}H-signals under usual experimental conditions, we estimated the free

activation energy ($\Delta G^{\ddagger}$) to be *ca.* 2.1 x10^3 cal/mol (25 °C) in a reported way[11] with assist from an NMR spectral simulation study. The 5-nitro compound (**9a**) is considered to have higher activation energy, since **9a** did not give unified signals even at 50 °C. It is apparent that the stability of the rotational isomers can be modulated with the 5-substituting groups and analyzed easily with an established NMR spectral method.

For the NMR spectral analysis, the 2-*t*-Bu and 2-Me groups will have a diagnostic value. For example, they can give strong singlet signals separated from each other and also from the other Me (Ac and Et) signals. Their chemical shifts are sensitive to the atropisomerism, and this property stands in contrast with that of the 5-NHAc signal of **5a** giving no split signal (Figure 4a). The difference arises from the space geometry of the 2-*t*-Bu and 2-Me groups relative to the 4-carbamide group (Scheme 3). The rotational restriction around the Ph-C=O single bond gives rise to a pair of *anti*- and *syn*-types of atropisomers as depicted in Scheme 3. The 2-*t*-Bu group and 2-Me groups are located in either an *anti*- or a *syn*-relation with the diethylamide. Therefore, they give the separated signals as observed in Figure 4. On the other hand, the signal of the 5-NHAc group in a coplanar relation with the aromatic ring becomes less sensitive to the *syn*- and *anti*-relation.

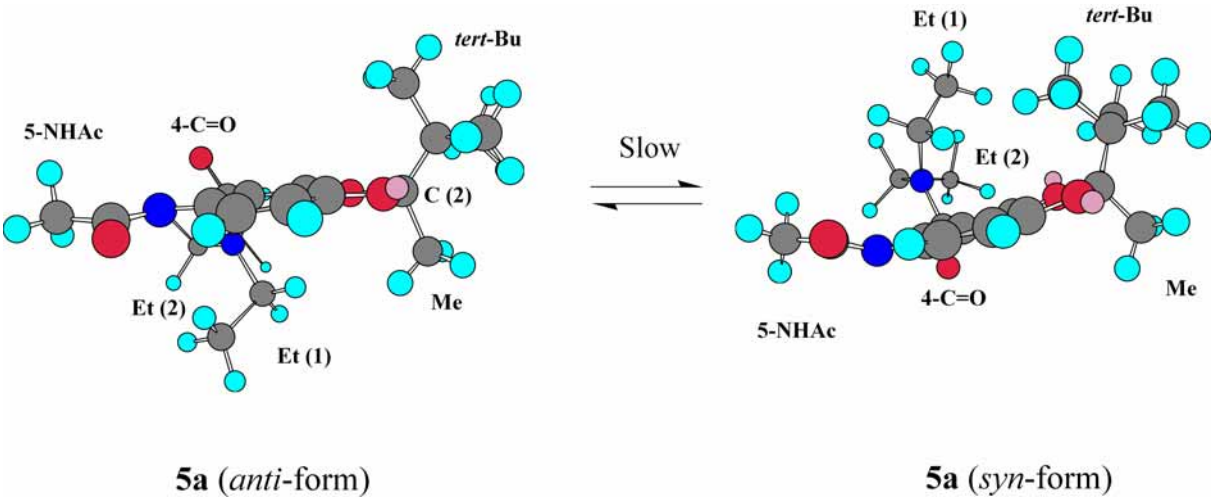

Scheme 3. Atropisomerism of **5a** giving two different molecular geometries with respect with the C-2 substituting groups (2-Me and 2-*t*-Bu). [The *syn*- and *anti*-isomers are defined tentatively with a spatial geometry between 2-*t*-Bu and diethylamide groups].

*4. Self-association property of γ-peptide models [(**4b**) and (**5b**)]*

In the case of the γ-peptide models [(**4b**) and (**5b**)] having two amide linkages in a separated position, they are not allowed to form an intramolecular H-bond across the peptide linkage. They showed no

atropisomerism in the ^{1}H NMR spectral studies conducted at 25°C in $CDCl_3$ (500 MHz). In this respect, their conformation properties may conform to those of **6** and **8** having no substituting group at the C-5 position. In ^{1}H NMR spectra, the 6-NH-CO signals of both **4b** and **5b** shifted to an upper-field (8.38 and 8.56 ppm) compared with the 5-NH-CO signals of **4a** (11.99 ppm) and **3a** (10.62 ppm). The chemical shifts should be usual to Ph-NHCO signals having no intra-molecular H-bond. The 4-CO-NH- signal of **4b** appeared in a region close to that of **6**, showing the existence of the coplanar conformation around the *C*-terminal linkage with the intramolecular H-bond. The UV bands in Figure 1 showed **4b** and **5b** have conjugated and non-conjugated structures at the Ph-carbonyl group, respectively. Also from the chemical shift of H-5 signals, we can predict the difference in conformation between **4b** and **5b**.

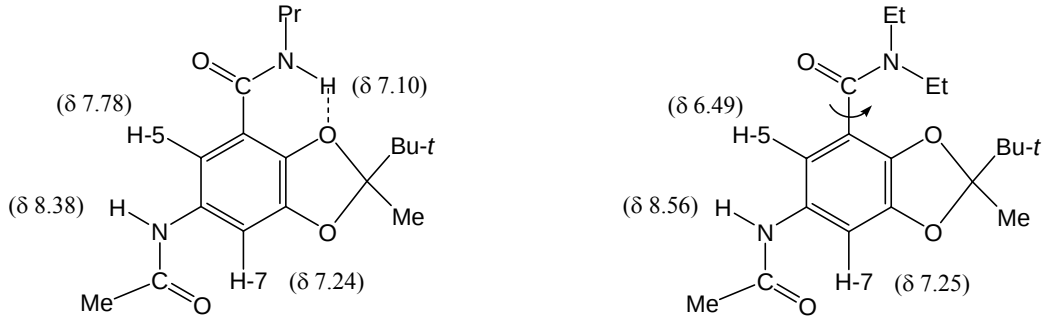

4b **5b**

Figure 5. Selected ^{1}H NMR spectral data of secondary and tertiary γ-peptide models (500 MHz, $CDCl_3$ at 25 °C)

Table 1 Concentration effect on ^{1}H-chemical shift [Δ ppm (48 mM – 4.8 mM)][a]

Compound	5- or 6-NHCO-	4-CONH-	Ac	Me	t-Bu	H-5	H-6	H-7
β-peptide models								
4a	+0.001	+0.000	+0.000	+0.001	+0.000	-	+0.000	+0.000
5a	+0.098	-	-0.007	-0.001	+0.002	-	-0.059	-0.009
γ-peptide models								
4b	+0.867	+0.058	+0.025	+0.001	+0.000	+0.076	-	+0.125
5b	+0.550	-	-0.042	-0.014	-0.007	-0.094	-	-0.025

[a] Measured at 500 MHz in $CDCl_3$ at 25 °C

The NMR spectral data in Table 1 and Figure 6 show that the ^{1}H-signals around the amide linkages change their chemical shifts at increasing concentration. Amide compounds are thought to show such concentration dependence due to either homo- or heterogeneous intermolecular H-bonding interactions.

In the present case, the dependence was largely different among the four peptide models. No substantial change was observed for **4a**. This can be rationalized by its stable intra-molecular H-bonds involved in both *C*- and *N*-terminal amide linkages. In the case of **5a** leaving the 5-acetamide group free from the H-bond, a notable change was observed in the chemical shifts of amide 5-NH-$COCH_3$ and aryl H-6. A more remarkable change was observed in the two γ-peptide models [(**4b**) and (**5b**)].

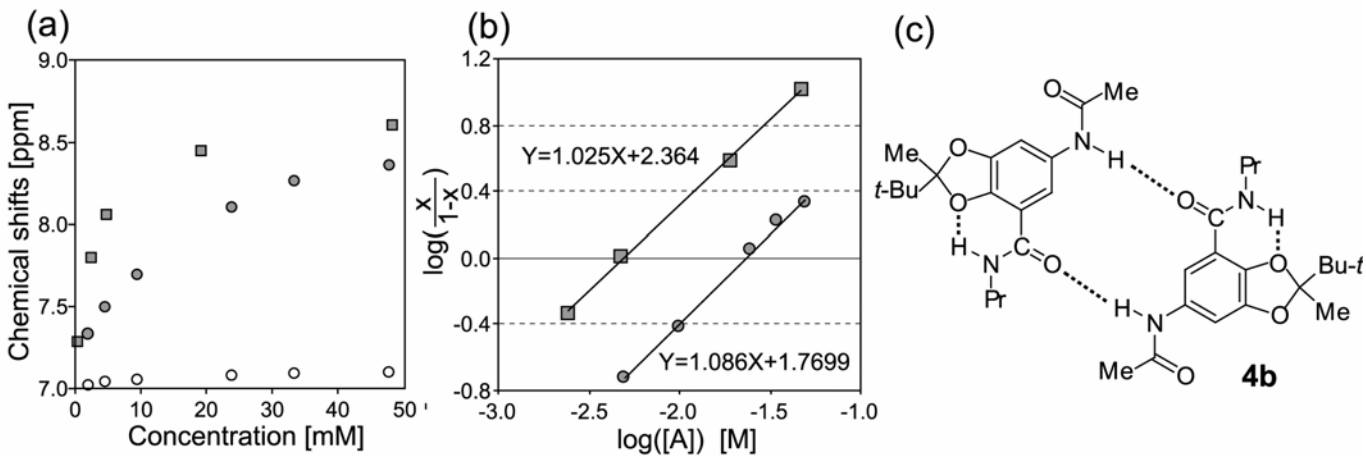

Figure 6. (a) Effects of concentrations on the chemical shift of –NH-CO signals of **4b** and **5b** [500 MHz in $CDCl_3$ at 25 °C: 4-CO-NH- (○) and 6-NH-CO- (●) of **4b**, 6-NH-CO- (■) of **5b**]. (b) Plots of concentrations in logarithm to chemical shift difference [6-NH-CO- (●) of **4b** and 6-NH-CO- (■) of **5b**] with a modified Hill's equation.[15] (c) A plausible self-association structure of **4b** with complementary intermolecular H-bonds.

In Figure 6a, the effect of concentration on each NH-CO signal in **4b** and **5b** is compared. It is obvious that the 6-NH-CO signals in both **4b** and **5b** [marked with (●) and (■)] permitted a larger effect than the 4-NH-CO signal of **4b** [(○)]. This supports that the 4-NH-CO proton in **4b** is engaged in a stable intramolecular H-bond, while the 6-NH-CO protons are associated with an intermolecular H-bond at high increased concentrations. From the saturation curves in Figure 6a, the self-association constants (*Ka*) of **4b** and **5b** were estimated to be 59 M^{-1} and 230 M^{-1}, respectively, in a reported way.[14] By adapting with Hill plots to a mode of self-association (Figure 6b),[15] we elucidated that the self-association of both **4b** and **5b** is based on 1:1 interaction [the number of interacting molecules (*n*) = 2.09 and 2.03]. Namely, these chemical shift changes arise from dimerization. The FAB-MS spectra of **4b** and **5b** gave mass ions corresponding to their dimer forms supporting the NMR analysis (EXPERIMENTAL).

From the chemical shift changes as described above, we assume such a self-association mechanism to **4b** that involves complementary intra- and intermolecular H-bonds (Figure 6c). The 6-NH-CO proton in **4b** is used for intermolecular H-bond with 4-C=O oxygen while keeping the intramolecular one between

4-CO-NH and *O*-3 atoms. As judged from the H-5 and H-7 signals moving to a down-field at higher concentrations, the self-association brings about a stable coplanar conformation around the 6-NHAc linkage.

To the dimer of **5b** having a non-coplanar conformation at the *C*-terminal, an alternative geometry may be deduced. At higher concentrations, the chemical shifts of H-5 and H-7 moved to an upper-field, that is, to an opposite direction to the case of **4b**. This means that **5b** tends to make its dimer taking a non-coplanar conformation also around the 6-NHAc linkage. Moreover, the 2-Me and 2-*t*-Bu signals of **5b** also showed a substantial concentration dependence. This means that suggests the 1,3-benzodioxole ring is also involved in the self-association. The *Ka* values have shown that the self-association of **5b** is stronger than that of **4b**. Thus, we may be able to image the dimer structure of **5b** in which the amide protons are making intermolecular hydrogen bonds in a similar manner to the case of **4.** Both of the amide linkages are, however, twisted to allow hydrophobic and/or $\pi - \pi$ interactions at the 1,3-benzodixole moiety.

SUMMARY

We have described that the designed 1,3-benzodioxole-based β- and γ-peptide linkages display unique fluorescence, conformation, and self-association properties each other. As demonstrated by **4a**, the secondary β-peptide linkage can be discriminated from the other types by its strong fluorescence, rigid conformation, and low self-association properties. The tertiary β-peptide linkage as those in **4b** can be characterized by its ability to make a pair of atropisomers. This owes to rotational restriction at the bulky *C*-terminal amide bond. The γ-peptide linkages as those in **4b** and **5b** show a notable dimerization property. When these properties are coupled with the instinct biological property of 1,3-benzodioxoles serving as antioxidant and antibacterial reagents, we will be able to design various bio- and chemo-functional conjugates. Along with our continuous studies on the design of artificial glycoconjugates, we have recently reported a series of chemo- and photo-reactive fluorescence labelling reagents,[7] which involve a photo-reactive fluorescent glycosylation donor.[8]

EXPERIMENTAL

Materials and Methods

^{1}H NMR spectra were recorded on Varian INOVA-500 (500MHz) at ambient temperature in $CDCl_3$ using TMS as an internal standard. UV (JASCO V-530), FL (JASCO FP777), and MS spectra (JAOL JMS-700) were recorded in conventional ways at room temperature. Nitronium tetrafluoroborate (0.5 M solution in

sulfolane) was purchased from Aldrich. Hexafluoropropene-diethylamine complex (HFPDA) was purchased from Tokyo Kasei Kogyo (Japan). 2-*tert*-Butyl-2-methyl-1,3-benzodioxole-4-carboxylic acid (**1**) was prepared with an established method from 3-methylcatechol.[9] The other chemicals and solvents were commercially available and used without further purification.

***N*-(*n*-Propyl)-2-*tert*-butyl-2-methyl-1,3-benzodioxole-4-carboxamide (6)**

A mixture of 2-*tert*-butyl-2-methyl-1,3-benzodioxole-4-carboxylic acid (**1**) (300 mg, 1.27 mmol) and HFPDA (660 mL, 1.91 mmol) in toluene (10 mL) was stirred for 1 h at ambient temperature. The mixture was washed with *sat.* $NaHCO_3$ and water, and then dried over $MgSO_4$. The filtrate was concentrated and purified by short silica gel column chromatography (toluene-ethyl acetate, 10: 1 (v/v)) to afford a carbonyl fluoride as a colorless syrup (297 mg, 98 %). ^{1}H NMR δ ppm: 1.092 (9H, s, *t*-Bu), 1.636 (3H, s, Me), 6.830 (1H, dt, *J*= 1.5 and 8.0 Hz, H-6), 6.957 (1H, dd, *J*= 1.0 and 8.0 Hz, H-7), 7.290 (1H, m, H-5); IR (KBr) 1840 (COF)

A solution of *n*-propylamine (147 mg, 2.48 mmol), triethylamine (250 mg, 2.48 mmol) and DMAP (13 mg, 0.10 mmol) in CH_2Cl_2 (3 mL) was cooled at 0 ˚C for 15 min. The carbonyl fluoride (297 mg, 1.24 mmol) in CH_2Cl_2 (2 mL) was added slowly at 0 ˚C and stirred at rt for 8 h. The reaction mixture was washed with *sat*. $NaHCO_3$ and water, and then dried over $MgSO_4$. After filtrating and evaporating, the residue was purified by silica gel column chromatography (toluene-ethyl acetate, 10: 1 (v/v)) to afford *n*-propylamide (**6**) as a white solid (325 mg, 94 %). mp 47 ˚C; ^{1}H NMR δ ppm: 1.000 (3H, t, *J*= 7.0 Hz, -$CH_2CH_2C\underline{H}_3$), 1.096 (9H, s, *t*-Bu), 1.629 (3H, s, Me), 1.637 (2H, m, -$CH_2C\underline{H}_2CH_3$), 3.383 and 3.510 (2H, m, -$C\underline{H}_2CH_2CH_3$), 6.841 (1H, dd, *J*= 1.5 and 7.5 Hz, H-7), 6.868 (1H, t, *J*= 7.5 Hz, H-6), 7.051 (1H, br s, -NH-), 7.518 (1H, dd, *J*= 2.0 and 7.5 Hz, H-5); HR-MS (FAB): calcd for $C_{16}H_{24}NO_3$ $[M+H]^+$: 278.1756; found 278.1758

***N*-(*n*-Propyl)-2-*tert*-butyl-2-methyl-5-nitro-1,3-benzodioxole-4-carboxamide (7a) and *N*-(*n*-Propyl)-2-*tert*-butyl-2-methyl-6-nitro-1,3-benzodioxole-4-carboxamide (7b)**

A solution of **6** (200 mg, 0.72 mmol) in MeCN (10 mL) was stirred at rt under nitrogen atmosphere for 15 min. NO_2BF_4 (0.5 M in sulfolane, 1.73 mL (0.86 mmol)) was added and the solution was stirred at the same temperature for 1 h. The mixture was poured into water (50 mL), and extracted with hexane-ethyl acetate (4:1, v/v). The combined extracts were washed with water and dried over $MgSO_4$. After filtrating and evaporating, the residue was purified by silica gel column chromatography (toluene-ethyl acetate, 10: 1 (v/v)) to afford 5-nitro compound (**7a**) (186 mg, 80 %) as a yellow solid together with 6-nitro compound (**7b**) (7 mg, 3 %) as a pale yellow crystal.

5-nitro compound (**7a**): mp 137 ˚C; ^{1}H NMR δ ppm: 1.009 (3H, t, *J*= 7.0 Hz, -$CH_2CH_2C\underline{H}_3$), 1.075 (9H, s, *t*-Bu), 1.640 (3H, s, Me), 1.664 (2H, m, -$CH_2C\underline{H}_2CH_3$), 3.461 (2H, m, -$C\underline{H}_2CH_2CH_3$), 5.904 (1H, br, -NH-), 6.754 (1H, d, *J*= 7.5 Hz, H-7), 7.647 (1H, d, *J*= 7.5 Hz, H-6); HR-MS (FAB): calcd for $C_{16}H_{23}N_2O_5$ $[M+H]^+$: 323.1607; found 323.1586

6-nitro compound: (**7b**) mp 99 ˚C; ^{1}H NMR δ ppm: 1.006 (3H, t, *J*= 7.5 Hz, -$CH_2CH_2C\underline{H}_3$), 1.117 (9H, s, tBu), 1.652 (2H, m, -$CH_2C\underline{H}_2CH_3$), 1.718 (3H, s, Me), 3.406 and 3.523 (2H, m, -$C\underline{H}_2CH_2CH_3$), 6.907 (1H, br, -NH-), 7.678 (1H, d, *J*= 2.5 Hz, H-7), 8.560 (1H, d, *J*= 2.5 Hz, H-5); HR-MS (FAB): calcd for $C_{16}H_{23}N_2O_5$ $[M+H]^+$: 323.1607; found 323.1595

***N, N*-Diethyl-2-*tert*-butyl-2-methyl-1,3-benzodioxole-4-carboxamide (8)**

Diethyl amide (**8**) was prepared, treating with diethylamine instead of *n*-propylamine, in the same way as for the preparation of **6**. (341 mg, 94 %, colorless syrup). ^{1}H NMR δ ppm: 1.067 (9H, s, tBu), 1.124 (3H, t, *J*= 6.5 Hz, -$CH_2C\underline{H}_3$), 1.232 (3H, t, *J*= 6.5 Hz, -$CH_2C\underline{H}_3$), 1.547 (3H, s, Me), 3.313 (1H, br m, -$C\underline{H}_2CH_3$), 3.590 (1H, br m, -$C\underline{H}_2CH_3$), 6.732 (1H, m, H-7), 6.784 (2H, m, H-5 and H-6); HR-MS(FAB) calcd for $C_{17}H_{26}NO_3$ $[M+H]^+$: 292.1913; found 292.1901

***N, N*-Diethyl-2-*tert*-butyl-2-methyl-5-nitro-1,3-benzodioxole-4-carboxamide (9a) and**
***N, N*-Diethyl-2-*tert*-butyl-2-methyl-6-nitro-1,3-benzodioxole-4-carboxamide (9b)**

5-Nitro compound (**9a**) and 6-nitro compound (**9b**) were prepared, starting from **8** (200 mg, 0.69 mmol), in the same way as for the preparation of **7a** and **7b**.

5-nitro compound (**9a**) (118 mg, 51 %, pale yellow crystal): mp 96 ˚C; ^{1}H NMR δ ppm: 1.065 and 1.079 (9H ×2, s ×2, *t*-Bu), 1.136 and 1.155 (3H ×2, t ×2, *J*= 7.5 Hz, -$CH_2C\underline{H}_3$), 1.287 (3H, t, *J*= 7.0 Hz, -$CH_2C\underline{H}_3$), 1.621 and 1.623 (3H ×2, s ×2, Me), 3.240 and 3.247 (2H ×2, m ×2, -$C\underline{H}_2CH_3$), 3.456 and 3.530 (1H ×2, m ×2, -$C\underline{H}_2CH_3$), 3.731 (1H, m, -$C\underline{H}_2CH_3$), 6.752 and 6.758 (1H×2, d ×2, *J*= 9.0 Hz, H-7), 7.836 and 7.844 (1H ×2, d ×2, *J*= 9.0 Hz, H-6); HR-MS(FAB) calcd for $C_{17}H_{25}N_2O_5$ [M+H]+: 337.1763; found 337.1721

6-nitro compound (**9b**) (97 mg, 42 %, pale yellow syrup): ^{1}H NMR δ ppm: 1.085 (9H, s, *t*-Bu), 1.160 (3H, t, *J*= 7.5 Hz, -$CH_2C\underline{H}_3$), 1.254 (3H, t, *J*= 7.0 Hz, -$CH_2C\underline{H}_3$), 1.633 (3H, s, Me), 3.292 (2H, br m, -$C\underline{H}_2CH_3$), 3.582 (2H, br m, -$C\underline{H}_2CH_3$), 7.591 (1H, d, *J*= 2.5 Hz, H-7), 7.876 (1H, d, *J*= 2.5 Hz, H-5); HR-MS(FAB) calcd for $C_{17}H_{25}N_2O_5$ $[M+H]^+$: 337.1763; found 337.1744

***N*-(*n*-Propyl)-5-acetamido-2-*tert*-butyl-2-methyl-1,3-benzodioxole-4-carboxamide (4a)**

5-nitro compound (**7a**) (100 mg, 0.31 mmol) was hydrogenated in methanol (5 mL) in the presence of 20 % $Pd(OH)_2$/C (5 mg) at rt under atmospheric pressure for 3 h. The reaction mixture was filtrated and

treated with acetic anhydride (0.5 mL, 5.28 mmol) at rt for 30 min. After evaporating, the residue was purified by silica gel column chromatography (toluene-ethyl acetate, 5:1 (v/v)) to afford compound (**4a**) as a white solid (99 mg, 95 %). mp 102 ˚C; ^{1}H NMR δ ppm: 1.012 (3H, t, *J*= 7.5 Hz, -$CH_2CH_2C\underline{H}_3$), 1.085 (9H, s, *t*-Bu), 1.614 (3H, s, Me), 1.653 (2H, m, -$CH_2C\underline{H}_2CH_3$), 2.183 (3H, s, Ac), 3.353 and 3.464 (2H, m, -$C\underline{H}_2CH_2CH_3$), 6.836 (1H, d, *J*= 9.0 Hz, H-7), 7.470 (1H, br s, -NH-), 8.190 (1H, d, *J*= 9.0 Hz, H-6), 11.992 (1H, br s, -NH-); HR-MS(FAB) calcd for $C_{18}H_{26}N_2O_4$ $[M]^+$: 334.1893; found 334.1923

***N*-(*n*-Propyl)-6-acetamido-2-*tert*-butyl-2-methyl-1,3-benzodioxole-4-carboxamide (4b)**

Compound (**4b**) was prepared, starting from **7b** (40 mg, 0.12 mmol), in the same way as for the preparation of **4a**. (41 mg, 95 %, white solid)

mp 188 ˚C; ^{1}H NMR δ ppm: 0.995 (3H, t, *J*= 7.0 Hz, -$CH_2CH_2C\underline{H}_3$), 1.087 (9H, s, *t*-Bu), 1.619 (3H, s, Me), 1.640 (2H, m, -$CH_2C\underline{H}_2CH_3$), 2.186 (3H, s, Ac), 3.371 and 3.488 (2H, m, -$C\underline{H}_2CH_2CH_3$), 7.105 (1H, br, -NH-), 7.243 (1H, d, *J*= 2.5 Hz, H-7), 7.786 (1H, d, *J*= 2.5 Hz, H-6), 8.377 (1H, br s, -NH-); HR-MS(FAB) calcd for $C_{18}H_{27}N_2O_4$ $[M+H]^+$: 335.1971; found 335.1925; LR-MS(FAB) 669 $[2M+H]^+$, 335 $[M+H]^+$, 277 $[M-57]^+$

***N, N*-Diethyl-5-acetamido-2-*tert*-butyl-2-methyl-1,3-benzodioxole-4-carboxamide (5a)**

Compound (**5a**) was prepared, starting from **9a** (120 mg, 0.36 mmol), in the same way as for the preparation of **4a**. (118 mg, 95 %, white solid)

mp 160 ˚C; ^{1}H NMR δ ppm: 1.049 and 1.063 (9H ×2, br s ×2, *t*-Bu), 1.134 (3H, br m, -$CH_2C\underline{H}_3$), 1.228 (3H, br t, *J*= 7.0 Hz, -$CH_2C\underline{H}_3$), 1.514 and 1.544 (3H ×2, br s ×2, Me), 2.089 (3H, s, Ac), 3.343 (2H, br m, -$C\underline{H}_2CH_3$), 3.578 (2H, m, -$C\underline{H}_2CH_3$), 6.719 (1H, d, *J*= 8.5 Hz, H-7), 7.318 and 7.368 (1H ×2, br d ×2, *J*= 8.5 Hz, H-6), 8.033 and 8.264 (1H ×2, br s ×2, -NH-); HR-MS(FAB) calcd for $C_{19}H_{29}N_2O_4$ $[M+H]^+$: 349.2127; found 349.2112

***N, N*-Diethyl-6-acetamido-2-*tert*-butyl-2-methyl-1,3-benzodioxole-4-carboxamide (5b)**

Compound (**5b**) was prepared, starting from **9b** (60 mg, 0.18 mmol), in the same way as for the preparation of **4a**. (60 mg, 96 %, colorless syrup)

^{1}H NMR δ ppm: 1.045 (9H, s, *t*-Bu), 1.122 (3H, t, *J*= 7.0 Hz, -$CH_2C\underline{H}_3$), 1.227 (3H, t, *J*= 7.0 Hz, -$CH_2C\underline{H}_3$), 1.515 (3H, s, Me), 2.090 (3H, s, Ac), 3.313 (2H, m, -$C\underline{H}_2CH_3$), 3.553 (2H, m, -$C\underline{H}_2CH_3$), 6.486 (1H, d, *J*= 2.5 Hz, H-7), 7.262 (1H, d, *J*= 2.5 Hz, H-6), 8.687 (1H, br s, -NH-); HR-MS(FAB) calcd for $C_{19}H_{28}N_2O_4$ [M+H]+: 349.2127; found 349.2099; LR-MS(FAB) 697 $[2M+H]^+$, 349 $[M+H]^+$, 291 $[M-57]^+$

ACKNOLEDGMENT

This study was supported by the 21st Century COE program "Nature-Guided Materials Processing" of Nagoya University from the MEXT of the Japanese Government, Grant-in-Aid for Scientific Research (B) (16350063), and Exploratory Research (16651107) of JSPS of the Japanese Government.

REFERENCES AND NOTE

1. R. Joshi, M. S. Kumar, K. Satyamoorthy, M. K. Unnikrisnan, and T. Mukherjee, *J. Agric. Food. Chem.*, 2005, **53**, 2696. S. Ibn-Ahmed, M. Khaldi, F. Cheretien, and Y. Chapleur, *J. Org. Chem.*, 2004, **69**, 6722. S. Walia, S. Saha, and B. S. Parmar, *J. Chromatogr. A*, 2004, **1047**, 229.
2. S. Easwar and N. P. Argade, *Tetrahedron Asymmetry*, 2003, **14**, 333. D. Enders and M. Backes, *Tetrahedron Asymmetry*, 2004, **15**, 1813. S. Moulay and W. H. Daly, *Eur. Polym. J.*, 1997, **33**, 929. L. Fabbrizzi, M. Licchelli, S. Masheroni, A. Poggi, D. Sacchi, and M. Zema, *Inorg. Chem.*, 2002, **41**, 6129. N. Micale, M. Zappalà, and S. Grasso, *Il Farmaco*, 2003, **58**, 351.
3. For a review, H. Meguro, J. –H. Kim, C. Bai, Y. Nishida, and H. Ohrui, *Chirality*, 2001, **13**, 441. For applications, Y. Nishida, J. –H. Kim, H. Ohrui, and H. Meguro, *J. Am. Chem. Soc.*, 1997, **119**, 1484. H. Ohrui, E. Itoh, Y. Nishida, H. Horie, and H. Meguro, *Biosci. Biotech. Biochem.*, 1997, **61**, 392. C. Bai, H. Ohrui, Y. Nishida, and H. Meguro, *Anal. Biochem.*, 1997, **246**, 246.
4. M. Suzuki, Y. Nishida, Y. Ohguro, Y. Miura, A. Tsuchida, and K. Kobayashi, *Tetrahedron Asymmetry*, 2004, **15**, 159.
5. Y. Nishida, M. Suzuki, and K. Kobayashi, *Anal. Sci.*, 2001, **17**, 685.
6. Y. Nishida, H. Ohrui, H. Meguro, and C. Kabuto, *Anal. Sci.*, 1991, **7**, 349.
7. M. Suzuki, Y. Nishida, Y. Ohguro, and K. Kobayashi, *Heterocycles*, 2005, **65**, 1051.
8. M. Suzuki, Y. Ohguro, Y. Nishida, M. Miyamoto, and K. Kobayashi, *Let. Org. Chem.*, 2005, **2**, 323.
9. Y. Nishida, E. Itou, M. Abe, H. Ohrui, and H. Meguro, *Anal. Sci.*, 1995, **11**, 213.
10. G. A. Olah and H. C. Lin, *J. Am. Chem. Soc*., 1974, **96**, 549.
11. D. Casarini, L. Lunazzi, and D. Macciantelli, *J. Chem. Soc., Perkin Trans. 2*, 1992, 1363.
12. J. Clayden, M. N. Kenworthy, L. H. Youssef, and M. Helliwell, *Tetrahedron Lett.*, 2000, **41**, 5171. J. Clayden, *Angew. Chem., Int. Ed. Engl*., 1997, **36**, 949. J. Clayden, L. W. Lai, M. Helliwell, *Tetrahedron*, 2004, **60**, 4399.
13. D. P. Curran, G. R. Hale, S. J. Geib, A. Balog, Q. B. Cass, A. L. G. Degani, M. Z. Hernandes, and L. C. G. Freitas, *Tetrahedron Asymmetry*, 1997, **8**, 3955. O. Kitagawa, H. Izawa, and T. Taguchi, *Tetrahedron Lett*., 1997, **38**, 4447.
14. M. Saunders and J. B. Hyne, *J. Phys. Chem.*, 1958, **29**, 1319. Y. Hamuro and A. D. Hamilton, *Bioorg. Med. Chem.*, 2001, **9**, 2355.
15. The number (*n*) of interacting molecules in the assumed self-association was analyzed in a following

way:

$$\underbrace{A + A + \cdots + A}_{n} \rightleftharpoons An$$

(1) $K = [An] / [A]^n$

(2) $x = [An] / ([A] + [An]) = \Delta\delta / \Delta\delta_{max}$

Equations (1) and (2) give equations in (3)

(3) $K[A]^{n-1} = x / (1-x)$ and $\log (x / 1-x) = (n-1)\log([A]) + \log K$

Here, n is the number (n) of self-associating molecules (A) reversibly with a constant (K) and $\Delta\delta$ is chemical shift change at the concentration [A].